INTERNATIONAL JOURNAL OF HYDROGEN ENERGY 45 (2020) 27891–27903

Available online at www.sciencedirect.com

ScienceDirect

journal homepage: www.elsevier.com/locate/he

Kinetic modeling investigation on the coupling effects of H_2 and CO_2 addition on the laminar flame speed of hydrogen enriched biogas mixture

Zhilong Wei [a], *Zhen He* [a], *Haisheng Zhen* [a,*], *Xiaosong Zhang* [a], *Zhenbin Chen* [a], *Zuohua Huang* [b]

[a] *Mechanical and Electrical Engineering College, Hainan University, China*

[b] *State Key Laboratory of Multiphase Flow in Power Engineering, Xian Jiaotong University, China*

HIGHLIGHTS

- Coupling effects of H_2 and CO_2 on S_L were isolated and analyzed.
- H_2 chemical effects result in the reduced dropping trend of S_L via R84 and R3.
- CO_2 chemical effects dominate the more evident decrease of S_L at the rich condition.
- R3, R46, R52, R84, R99 and R158 have major contributions on the chemistry transition.
- H_2/CO_2-related chemistry can be monitored directly by R84 and R99.

ARTICLE INFO

Article history:
Received 14 May 2020
Received in revised form
11 July 2020
Accepted 13 July 2020
Available online 2 August 2020

Keywords:
Biogas-hydrogen fuel
Coupling effects of H_2 and CO_2
Laminar flame speed
Reaction pathway

ABSTRACT

The numerical simulation was conducted to investigate the coupling effects of H_2 and CO_2 on the laminar flame speed and reaction pathways of the biogas-hydrogen mixtures. The same proportions of H_2 and CO_2 were considered in the study. The dilution effects, chemical effects and thermal effects of H_2 and CO_2 were isolated, while the contributions of different effects were also calculated to identify the dominating factor. The results show that H radical pool plays the important role in the variation of laminar flame speed of biogas-hydrogen mixture. The coupling dilution effects of H_2 and CO_2 lead to the considerable decrease of H radical and dominate the decreased laminar flame speed. The H_2 chemical effects improve R84 ($OH + H_2 = H_2O + H$) and R3 ($O + H_2 = H + OH$) quite effectively, which results in the reduced dropping trends of H radical and laminar flame speed from BG60H40 to BG40H60. The CO_2 chemical effects suppress the major H radical production reactions of R84, R3, R99 ($OH + CO = H + CO_2$) and R10 ($O + CH_3 = H + CH_2O$) more apparently at the fuel-rich condition, while importance of major consumption reactions (R53: $H + CH_4 = CH_3 + H_2$, R52: $H + CH_3(+M) = CH_4(+M)$ and R58: $H + CH_2O = HCO + H_2$) are higher at the fuel-rich condition. This dominates the more evident decrease of H radical and laminar flame speed at the fuel-rich condition. Based on the ROP analysis, R3, R46 ($H + HO_2 = 2OH$), R52, R84, R99 and R158 ($2CH_3(+M) = C_2H_6(+M)$) have the major contributions on the chemistry transition caused by the coupling effects of H_2 and CO_2. The decreased contribution of R158 and R99 indicate the weakened CH_4-related chemistry while the increased contributions of R3, R46, R52 and R84 indicate the improved H_2-related chemistry in the biogas-hydrogen flame. Furthermore, coupling effects of H_2

* *Corresponding author.*
E-mail address: ban18@126.com (H. Zhen).

https://doi.org/10.1016/j.ijhydene.2020.07.119

and CO_2 or H_2/CO_2-related chemistry can be monitored by the contribution variations of R84 and R99 on the OH radical concentration.

Introduction

The serious environmental challenges and the increasing world consumption of fossil energy have prompted much more efforts to be made so as to develop sustainable and renewable fuels in recent decades. Biogas (BG) is considered as a promising renewable clean fuel due to its short carbon cycle and its easy productivity. Since biogas is the product of the fermentation of agriculture wastes, animal wastes and other sources of biomass, it consists of methane (CH_4), carbon dioxide (CO_2) and a small amount of oxygen, nitrogen and other organic compounds. Thanks to the various sources, the CO_2 content in the biogas varies between 40% and 80% generally. The considerable amount of inert CO_2 in the biogas leads to its lower heating value, decreased laminar flame speed and worse combustion stability. The real utilization of biogas is thus restricted considerably in industrial facilities [1,2]. Hydrogen (H_2), as a carbon-free gaseous fuel, has been widely accepted as an almost perfect clean energy and has a promising prospect in combustion engineering. Thanks to its high reactivity and diffusivity, hydrogen has the excellent mass-basis calorific value, the low minimum ignition energy, extensive flammability and the quite high flame propagation speed [3–6]. This makes the hydrogen to be an excellent addition to improve combustion characteristics of other hydrocarbon fuels, such as methane, propane and LPG [7–12]. Therefore, the hydrogen addition can also be adopted to improve the fuel characteristics of biogas and improve its practical applications.

To better utilize the biogas-hydrogen blends, effects of H_2 and CO_2 on the combustion features of biogas-hydrogen blends need to be studied thoroughly. In the past few decades, several researches have been conducted to improve the understandings of fuel characteristics of biogas-hydrogen blends. Leung et al. [13] reported that the stability range of the biogas diffusion flame can be improved effectively with a small amount of hydrogen addition. Chen and Zheng [14] performed the numerical simulations to study the mild combustion characteristics of biogas-hydrogen mixture and suggested that the lower preheated temperature is preferred for obtaining the stable mild combustion of biogas-hydrogen mixture. Zhang et al. [15] conducted an experiment to investigate the effects of hydrogen addition on the biogas combustion stability in a spark ignited engine and found that the hydrogen addition can enhance the heat release rate and improve the combustion stability of the biogas fuel. Hu et al. [16] reported that the increased hydrogen addition can increase the hydrodynamic and thermal mass diffusion instability in the biogas-hydrogen spherical flame. Zhang et al. [16] evaluated the fuel variability effects on the biogas-hydrogen combustion and suggested that the flame speed fluctuation is caused by the hydrogen variability primarily. Wei et al. [17] conducted the experiment to analyze the effects of H_2 and CO_2 on the impingement heat transfer of the biogas-hydrogen flame and proposed an optimum hydrogen addition to improve the heat transfer of biogas-hydrogen impinging flame. Zhen et al. [18] investigated heat transfer and flame configurations of the hydrogen enriched biogas flame systematically. Zhen et al. [19] also performed an experimental study on the stability of biogas-hydrogen diffusion flame and reported that the hydrogen addition accelerates the fuel mass diffusion and improves the stability of biogas diffusion flame.

Besides, the heat release features [20], emission formations [21–23], explosion characteristics [24] and self-acceleration [25] of biogas-hydrogen combustion are studied by some researchers, while the combustion performance of biogas-hydrogen blends in the real combustors are investigated in plenty of studies [26–29]. The above mentioned studies provide quite a lot valuable information of the combustion features of biogas-hydrogen blends. Whereas, it is general that H_2 effects and CO_2 effects are investigated separately in the previous studies. Considering the simultaneous existence of H_2 and CO_2 in the biogas-hydrogen blend and their extremely different features to affect the combustion process, it is quite critical to identify the coupling effects of H_2 and CO_2 on the combustion characteristics of the biogas-hydrogen blend. This can help to obtain a deeper understanding on the combustion characteristics of biogas-hydrogen blends and further improve its practical applications. Hence, more studies need to be conducted to investigate the coupling effects of H_2 and CO_2 on the combustion features of biogas-hydrogen blend.

As one of most significant global combustion parameters, the laminar flame speed is not only quite pivotal for the development of the chemical mechanism and determination of turbulent burning velocity but also helpful for the design and optimization of combustion facilities. However, the laminar flame speed of biogas-hydrogen-air mixture are reported by few studies and the limited range of conditions are considered in these studies [30–34]. Furthermore, the coupling effects of H_2 and CO_2 on the laminar flame speed of biogas-hydrogen blends are rarely investigated. Considering the promising prospect of biogas-hydrogen blends and the significance of laminar flame speed on its real applications, there exists an urgent need to carry out the investigation on the coupling effects of H_2 and CO_2 on the laminar flame speed of the biogas-hydrogen blend. Based on our previous experimental work [33], the coupling effects of H_2 and CO_2 on the laminar flame speed will be further analyzed quantitatively with the numerical simulation in this study.

The objective of this research is to investigate the coupling effects of H_2 and CO_2 on the laminar flame speed of biogas-hydrogen blend. To better complete this objective, the

proportion of H_2 will keep the same with the CO_2 proportion and the proportions of H_2 and CO_2 will be varied simultaneously. Furthermore, dilution, thermal and chemical effects of H_2 and CO_2 will be isolated simultaneously to identify the dominating factor in the coupling effects of H_2 and CO_2. In addition, the change of reaction pathway will be investigated based on the rate of production (ROP) analysis, which can improve the understanding on the chemistry transition process from methane to the biogas-hydrogen blend when H_2 and CO_2 are added simultaneously.

Numerical methods

In this study, the biogas was emulated by mixing CH_4 and CO_2 according to the volumetric ratios of 80%: 20%, 60%: 40% and 40%: 60%, which are denoted as BG80, BG60 and BG40, respectively. In addition, the hydrogen addition is defined as $\alpha H_2 = V_{H2}/(V_{CH4}+V_{CO2})$, where V_{H2}, V_{CH4} and V_{CO2} are the mole fractions of hydrogen, methane and carbon dioxide, respectively. To better analyze the coupling effects of H_2 and CO_2, $\alpha H_2 = 20\%$, 40% and 60%, which are the same as the volumetric ratios of CO_2, were added into BG80, BG60 and BG40 respectively in the study, and the obtained biogas-hydrogen mixtures are denoted as BG80H20, BG60H40 and BG40H60, respectively. The details of the compositions of biogas-hydrogen mixtures used in this study are given in Table 1.

By using the PREMIX code [35] of CHEMKIN-II and the GRI 3.0 mechanism [36], the laminar flame speeds of CH_4 and biogas-hydrogen mixtures were calculated at 298 K and 1 atm under three equivalence ratios (ϕ = 0.9, 1.0 and 1.1), and the multicomponent transport and Soret effect were both included in the model. The adaptive grid control on solution gradient (GRAD) and adaptive grid control on solution curvature (CURV) were set to 0.05 and 0.05, respectively. GRI 3.0, which consists of 53 species and 325 elementary chemical reactions, has been demonstrated to be an accurate detailed mechanism to describe the methane combustion by a few of experimental data. To confirm the accuracy of GRI 3.0 on the biogas-hydrogen mixture, the laminar flame speed measured by the cylindrical combustion bomb [33] are adopted here to compare the calculated results. The measured and calculated laminar flame speeds of biogas-hydrogen mixture are illustrated in Fig. 1. It is seen that the calculated results can agree well with the measured data, which indicates that GRI 3.0 can be used for the further investigation of combustion characteristics of biogas-hydrogen mixture.

In order to investigate the coupling effects of H_2 and CO_2 thoroughly, the dilution, thermal and chemical effects of H_2 and CO_2 were separated in the study by introducing the fictitious H_2 and CO_2, referred to FH_2 and FCO_2, respectively. FH_2 and FCO_2 have the same thermodynamic properties, transport properties and third-body collision efficiencies as the normal H_2 and CO_2, but they are not allowed to participate in any chemical reactions. To isolate the dilution, thermal and chemical effects of H_2 and CO_2, the CH_4, $CH_4/N_2/N_2$, $CH_4/N_2/FH_2$, $CH_4/FCO_2/FH_2$, $CH_4/FCO_2/H_2$ and $CH_4/CO_2/H_2$ were calculated successively at a condition. Based on these calculations, the difference between CH_4 and $CH_4/N_2/N_2$ is attributed to the coupling dilution effects of H_2 and CO_2 (Coupling D). The difference between $CH_4/N_2/N_2$ and $CH_4/N_2/FH_2$ is resulted from the thermal effects of H_2 (H2 T) while difference between $CH_4/N_2/FH_2$ and $CH_4/FCO_2/FH_2$ is ascribed to the thermal effects of CO_2 (CO2 T). Furthermore, the chemical effects of H_2 (H2 C) can be obtained by the difference between $CH_4/FCO_2/FH_2$ and $CH_4/FCO_2/H_2$ while the chemical effects of CO_2 (CO2 C) can be calculated by the difference between $CH_4/FCO_2/H_2$ and $CH_4/CO_2/H_2$. With these results, different effects of H_2 and CO_2 on the laminar flame speed can be investigated clearly, while the importance of different effects of H_2 and CO_2 can be also identified.

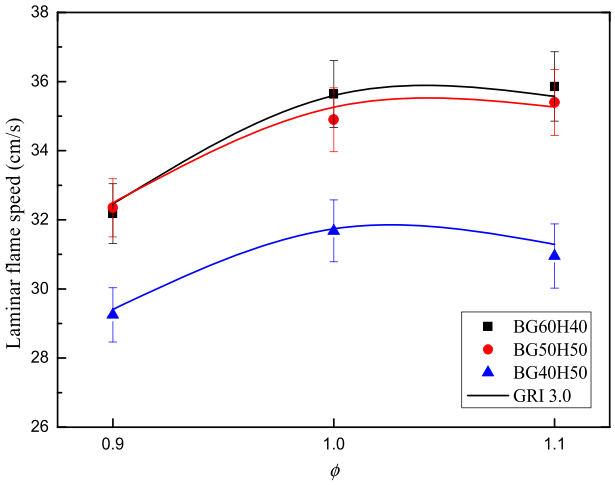

Fig. 1 – The comparison of calculated results and measured data of biogas-hydrogen flames.

Table 1 – The details of fuel compositions considered in this study.

	Mole fraction		
	CH_4	CO_2	H_2
CH_4	1	0	0
BG80H20	0.666	0.167	0.167
BG60H40	0.428	0.286	0.286
BG40H60	0.25	0.375	0.375

Results and discussions

Coupling effects on the laminar flame speed

The laminar flame speeds of biogas-hydrogen mixtures are compared with that of methane at ϕ = 0.9, 1.0 and 1.1 as illustrated in Fig. 2. It is seen that, with the increased proportions of H_2 and CO_2, the laminar flame speeds of biogas-hydrogen mixture are decreased steadily from the methane to the BG60H40 mixture. However, with the further increased percentages of H_2 and CO_2, the laminar flame speed of BG40H60 mixture is increased considerably at the fuel-lean condition but still decreased slightly at the fuel-rich condition compared with that of BG60H40 mixture. Considering the variation of laminar flame speed, it seems that the increased CO_2 content contributes to the dropping trend of the laminar

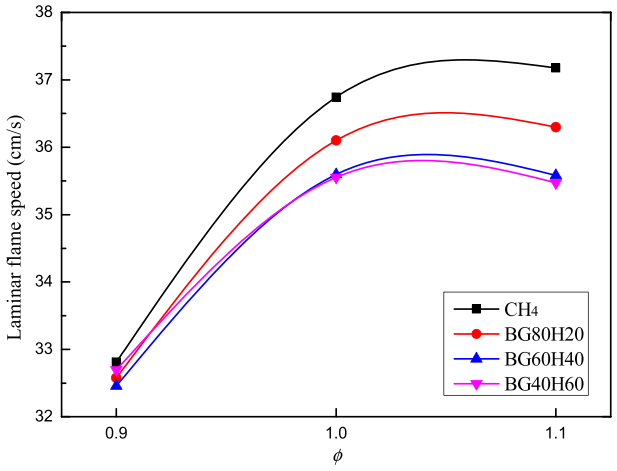

Fig. 2 – The laminar flame speeds of methane and biogas-hydrogen mixtures at $\phi = 0.9$, 1.0 and 1.1.

flame speed firstly while the effects of H_2 will overcome the effects of CO_2 and reduce the dropping trend of laminar flame speed of the BG40H60 mixture.

To better investigate the coupling effects of H_2 and CO_2, the variations of laminar flame speed caused by the coupling dilution effects of H_2 and CO_2, and the respective thermal and chemical effects of H_2 and CO_2 are isolated and given in Fig. 3. As shown in Fig. 3, there is no surprise that the chemical effects of CO_2 decrease the laminar flame speed while the chemical effects of H_2 can increase the laminar flame speed quite efficiently. In addition, it is seen that the thermal effects of CO_2 can affect the laminar flame speed more evidently than that of H_2 owing to its much larger specific heat capacity which decreases the flame temperature. Thus the H_2 reactivity dominates the coupling chemical effects while the thermal properties of CO_2 give rise to its more significant role in the coupling thermal effects. In addition, the coupling dilution effects of H_2 and CO_2 play the most important role in the decrease of laminar flame speed of biogas-hydrogen mixture. Besides, it is seen that the dilution, thermal and chemical effects of H_2 and CO_2 are increased considerably with their increased proportions, while H_2 and CO_2 can exert more evident influences on the laminar flame speed at the fuel-rich condition than that at the fuel-lean condition thanks to their higher proportions in the unburned gases mixture. Overall, it is known that the coupling dilution effects of H_2 and CO_2 dominate the decrease of laminar flame speed with the increased proportions of H_2 and CO_2, while the chemical effects of H_2 play the critical role in the increase of laminar flame speed.

The laminar flame speed variation is normalized by the sum of the absolute values of laminar flame speed variations caused by different effects at a condition, which can compare the relative importance of dilution, thermal and chemical effects of H_2 and CO_2 at different conditions clearly. The obtained results are shown in Fig. 4. With the increased H_2 and CO_2 contents, the contribution of CO_2 chemical effect is decreased while that of H_2 chemical effect is increased at either the fuel-lean or the fuel-rich condition. In addition, the thermal effects of H_2 and CO_2 both become less important in the variation of laminar flame speed while the significance of coupling dilution effects of H_2 and CO_2 is enhanced from CH_4 to BG40H60. Besides, it is noted that the contributions of CO_2 chemical effects are increased by around 30% at the fuel-rich condition compared with that at the fuel-lean condition while the contributions of other factors are decreased slightly at the fuel-rich condition. Hence, compared with that at $\phi = 0.9$, CO_2 chemical effects play the more significant role in the laminar flame speed at $\phi = 1.1$ as shown in Fig. 4.

The total contributions of positive (thermal and chemical effects of H_2) and negative (thermal and chemical effects of CO_2 and coupling dilution effects) effects on the laminar flame speed are shown in Fig. 5. It is seen that the negative effects account for more than 50% of coupling effects of H_2 and CO_2 on the laminar flame speed, which means that the negative effects of H_2 and CO_2 dominate the variation of laminar flame speed of the biogas-hydrogen mixture and result in the dropping trend of laminar flame speed from CH_4 to biogas-hydrogen mixture as shown in Fig. 2. In addition, it is noted that the contribution of positive effects of H_2 and CO_2 suffer

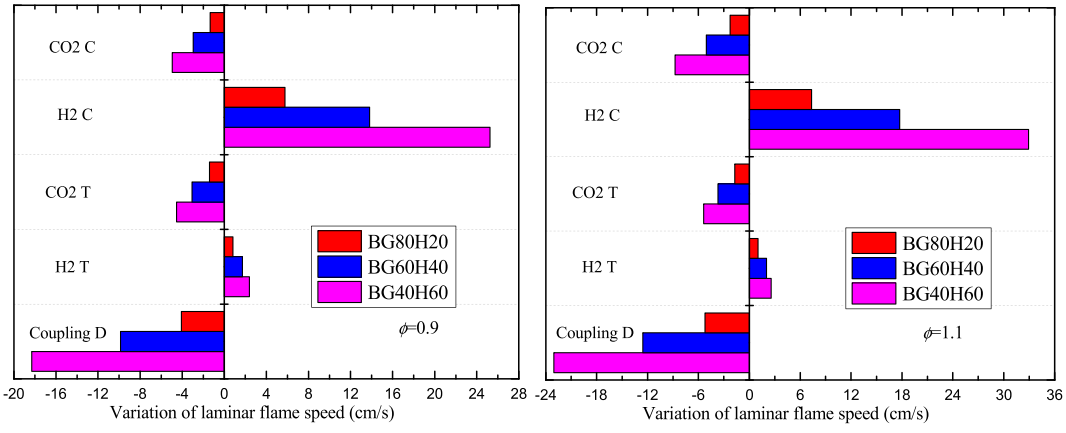

(a) ϕ=0.9 (b) ϕ=1.1

Fig. 3 – The coupling dilution effect and respective thermal/chemical effects of H_2 and CO_2 on laminar flame speeds of biogas-hydrogen mixtures at $\phi = 0.9$ and 1.1.

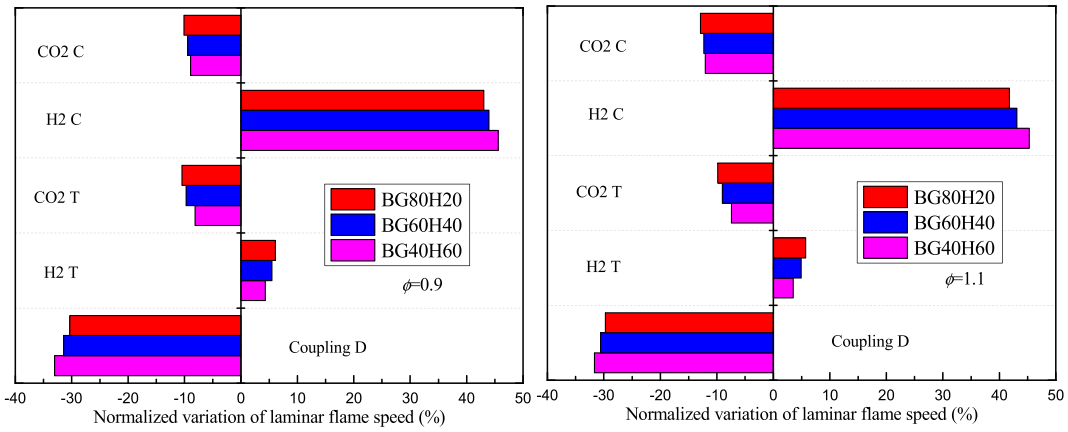

(a) ϕ=0.9 (b) ϕ=1.1

Fig. 4 – The contributions of different effects of H_2 and CO_2 on laminar flame speeds of biogas-hydrogen mixtures at $\phi = 0.9$ and 1.1.

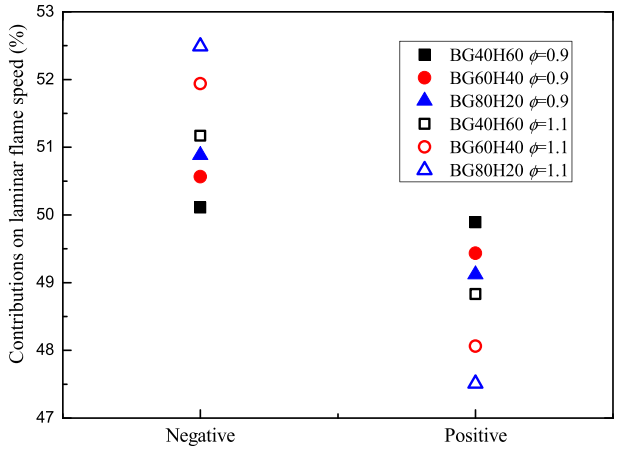

Fig. 5 – The total negative and positive effects of H_2 and CO_2 on laminar flame speeds of biogas-hydrogen mixtures at $\phi = 0.9$ and 1.1.

the more evident increase from BG60H40 to BG40H60 compared with that from BG80H20 to BG60H40 at $\phi = 0.9$ and 1.1 as shown in Fig. 5. This indicates that the positive effects of H_2 and CO_2 are improved more effectively than the negative effects in the BG40H60 mixture. Furthermore, the contribution of H_2 thermal effects is decreased with the increased H_2 and CO_2 as shown in Fig. 4, the more efficient improvements of positive effects in the BG40H60 flame are thus resulted from the more effectively increased contribution of H_2 chemical effects. This finally leads to the considerably reduced dropping rate of laminar flame speed from BG60H40 to BG40H60.

Besides, it is apparent that, as shown in Fig. 5, the negative effects of H_2 and CO_2 at the fuel-rich condition can be approximately 1%–1.5% higher than that at the fuel-lean condition. Considering the contributions of thermal/chemical effects of CO_2 and coupling dilution effects shown in Fig. 4, it is known that the higher contributions of CO_2 chemical effects bring about the increased negative effects at the fuel-rich condition. Consequently, compared with that at the fuel-lean condition, the much stronger CO_2 chemical effects at the fuel-rich condition give rise to the more evident decrease of laminar flame speed at $\phi = 1.1$ than that at $\phi = 0.9$ as shown in Fig. 2. In addition, combined with the more obvious improvements on the positive effects from BG60H40 to BG40H60, the stronger negative effects at the fuel-rich condition contribute to the slight decrease of laminar flame speed from BG60H40 to BG40H60 at $\phi = 1.1$ but the moderate increase at $\phi = 0.9$ as shown in Fig. 2.

Overall, it is concluded that the lower laminar flame speed of biogas-hydrogen mixture is dominated by the increased contribution of coupling dilution effects of H_2 and CO_2, while the more evident dropping trend of laminar flame speed at $\phi = 1.1$ is ascribed to the stronger suppressions caused by CO_2 chemical effects. From BG60H40 to BG40H60, the reduced dropping trend of laminar flame speed is attributed to the more evidently increased contribution of H_2 chemical effect, while the lower contribution of CO_2 chemical effects at the fuel-lean condition further result in the increased laminar flame speed at $\phi = 0.9$ as shown in Fig. 2.

Coupling effects on the radical pool

The radical pool has the close relationship with the laminar flame speed that can be used to further clarify the reasons of the laminar flame speed variation. The radical pool of the methane flames and biogas-hydrogen flames are plotted in Fig. 6. As shown in Fig. 6, OH radical is the most abundant radical in the radical pool at the fuel-lean condition while H racial is more significant at the fuel-rich condition. In addition, the peak mole fractions of H, O, OH and CH_3 are decreased generally from CH_4 to BG40H60. It is noted that the H radical can be an indicator of the laminar flame speed of the biogas-hydrogen mixture because it peak mole fraction can reflect the variation of laminar flame speed reasonably. Specifically, the peak mole fraction of H radical shows a quite moderate dropping trend at the fuel-lean condition compared with that at the fuel-rich condition as shown in Fig. 6. Furthermore, the peak mole fraction of H radical is increased

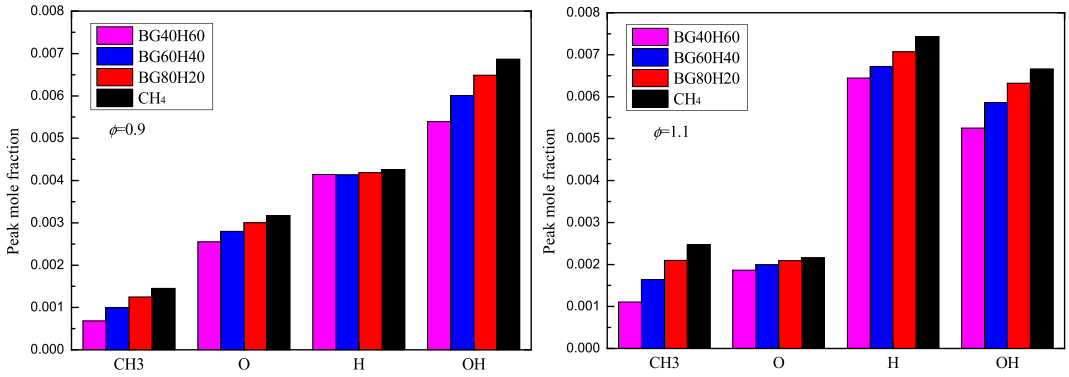

(a) ϕ=0.9 (b) ϕ=1.1

Fig. 6 – The radical pool (H, O, OH and CH_3) in the methane flames and biogas-hydrogen flames at $\phi = 0.9$ and 1.1.

slightly from 4.13×10^{-3} in the BG60H40 flame to 4.14×10^{-3} in the BG40H60 flame at $\phi = 0.9$ while its dropping trend becomes comparatively moderate from BG60H40 to BG40H60 at $\phi = 1.1$. Hence, the variations of H radical are consistent with the variations of laminar flame speed at $\phi = 0.9$ and 1.1 as shown in Fig. 2, which indicates that H radical should play the dominated role in the laminar flame speed of biogas-hydrogen flame. In addition, the considerably decreased CH_3 mole fraction indicates the weakened CH_4 chemistry [37].

To identify the different effects of H_2 and CO_2 on the H radical in the biogas-hydrogen flame, the peak mole fraction variations of H radical caused by the different effects of H_2 and CO_2 in the biogas-hydrogen mixture are illustrated in Fig. 7, while the contributions of different effects of H_2 and CO_2 on the H radical variation are shown in Fig. 8. As shown in Fig. 7, the peak mole fraction variation of H radical can be increased effectively with the increased percentages of H_2 and CO_2. However, the contributions of H_2 chemical effects and coupling dilution effects are increased from BG80H20 to BG40H60 while the contributions of other effects are decreased as shown in Fig. 8. In addition, it is seen that the contributions of CO_2 chemical effects on the H radical variation are higher at $\phi = 1.1$ than that at $\phi = 0.9$. It is thus confirmed that the slightly increased peak mole fraction of H radical from BG60H40 to BG40H60 at $\phi = 0.9$ can be attributed to the enhanced contribution of H_2 chemical effects while the steady decrease of peak mole fraction of H radical at $\phi = 1.1$ is dominated by the higher importance of CO_2 chemical effects at the fuel-rich condition.

The primary reactions to produce and consume the H radical in the CH_4 and BG40H60 flames are illustrated in Fig. 9 in order to further clarify the roles of H_2 and CO_2 in the variation of the H radical. In the methane and biogas-hydrogen flames, the primary reactions to produce the H radical are R84: $OH + H_2 = H_2O + H$, R3: $O + H_2 = H + OH$, R99: $OH + CO = H + CO_2$ and R10: $O + CH_3 = H + CH_2O$, while the major reactions to consume the H radical are R38: $H + O_2 = OH + O$, R52: $H + CH_3(+M) = CH_4(+M)$, R53: $H + CH_4 = CH_3 + H_2$ and R58: $H + CH_2O = HCO + H_2$. Furthermore, R84 and R38 are the most important reactions to produce and consume the H radical respectively at both fuel-lean and fuel-rich conditions. In addition, as shown in Fig. 9, the difference between the ROPs of CH_4 and $CH_4/FCO_2/FH_2$ is ascribed to the thermal and dilution effects of H_2 and CO_2. The difference between the ROPs of $CH_4/FCO_2/FH_2$ and $CH_4/FCO_2/H_2$ is resulted from the H_2 chemical effects while the difference between the ROPs of

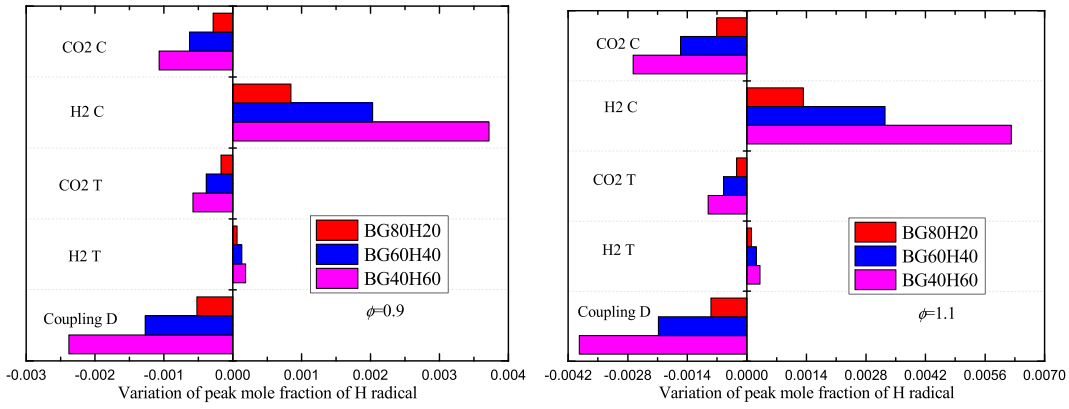

(a) ϕ=0.9 (b) ϕ=1.1

Fig. 7 – The coupling dilution effect and respective thermal/chemical effects of H_2 and CO_2 on the H radical of biogas-hydrogen mixtures at $\phi = 0.9$ and 1.1.

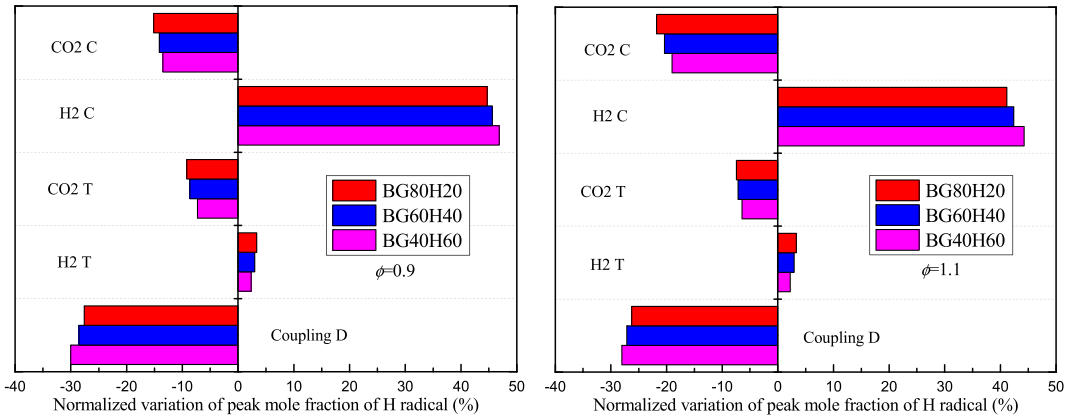

Fig. 8 – The contributions of different effects of H_2 and CO_2 on the H radical of biogas-hydrogen mixtures at $\phi = 0.9$ and 1.1.

$CH_4/FCO_2/H_2$ and BG40H60 is attributed to the CO_2 chemical effects. It is thus known that, as shown in Fig. 9, the coupling dilution and thermal effects of H_2 and CO_2 lead to the considerable decrease in ROPs of H radical for all major reactions thanks to the considerably decreased temperature and reduced active radicals. The coupling dilution effects of H_2 and CO_2 consequently contribute to the considerably decreased H radical in the radical pool and then suppress the flame propagation effectively.

As the H_2 chemical effects are introduced, the ROPs of H radical via these reactions are all improved effectively. Whereas, it is noted that the ROPs of R84, R3 and R52 are enhanced drastically in the $CH_4/FCO_2/H_2$ flame which are even higher than that in the CH_4 flame, while ROPs of R10, R53, R58 and R99 are still lower than that in the CH_4 flame as shown in Fig. 9. Besides, it is seen that, compared with that in the CH_4 flame, the H_2 chemical effects lead to the slightly lower ROP of R38 in the $CH_4/FCO_2/H_2$ flame at the fuel-lean condition but the higher ROP at the fuel-rich condition. With the introduced H_2 chemical effects, R84 and R38 can be improved considerably by the high reactivity of H_2 which can increase the amount of H, O and OH radicals considerably. This can then accelerate other reactions effectively and enhance the heat release rate of biogas-hydrogen combustion [20], which gives rise to the enhancements of ROPs of these reactions as shown in Fig. 9. Additionally, the quite evident improvements on the ROP of R84 and R3 are caused by the obviously increased amount of H_2 in the mixture and its direct participations in these two reactions. For R52, it is a three-body reaction which can be affected drastically by the concentrations of H, CH_3 and the third-body amount in the flame. The considerably increased H radical and the large amounts of the third-body (H_2, CO_2, H_2O, etc.) in the $CH_4/FCO_2/H_2$ flame can thus accelerate the R52 efficiently by the enhanced collision efficiency, which then brings about its higher ROP of H radical than that of CH_4 flame. Besides, the ROP of R38 in the $CH_4/FCO_2/H_2$ flame is slightly lower than that in the CH_4 flame at fuel-lean condition thanks to the abundant O_2 in the mixture while its ROP becomes moderately higher at the fuel-rich condition which can be ascribed to the quite higher concentration of H radical. Considering the more improvements on R84, R3 and R52, it is known that these three reactions play the more important roles in the H radical pool variation caused by the H_2 chemical effects. Although the higher ROP of R52 can accelerate the consumption of H radical in the flame, its consumption rate is much lower than the production rate of R84 and cannot overcome the improvements of R84 on the H radical production. As a result, the considerably improved R84 and R3 dominate the increased H radical with the H_2 chemical effects.

As the CO_2 chemical effects are further introduced, the ROPs of these reactions are decreased effectively in the BG40H60 flame at both the fuel-lean and the fuel-rich condition as shown Fig. 9. It is known that the CO_2 chemical effects can accelerate the reverse reaction of R99 directly, which can compete for the H radical with R38 significantly and then suppress this most significant chain-branching reaction in the biogas-hydrogen combustion [38,39]. In addition, R99 is an important exothermic reaction in the biogas-hydrogen mixture [20]. The CO_2 chemical effects can suppress the forward reaction of R99 and then decrease the heat release rate of the biogas-hydrogen combustion, which leads to the declined temperature in the reaction zone [40]. Hence, the suppressed chain-branching reaction and declined temperature caused by the CO_2 chemical effects can suppress the H radical production considerably. Furthermore, the importance of R52 on the H radical pool is increased in the biogas-hydrogen flame considering that its ROP is higher than that in the CH_4 flame while ROPs of other major H radical consumption reactions are lower than that in the CH_4 flame. The increased importance of R52 can be ascribed to the obvious improvements of H_2 chemical effects. As a result, with the CO_2 chemical effects, the suppressed H radical production and the increased contribution of R52 contribute to the decreased H radical with the CO_2 chemical effects.

Besides, thanks to the coupling chemical effects of H_2 and CO_2, the ROPs of R84 and R52 in the BG40H60 flame become higher than that in the CH_4 flame while the ROP of R3 in the BG40H60 flame is higher at the fuel-lean condition but slightly lower at the fuel-rich condition than that in the CH_4 flame as shown Fig. 9. For other reactions, their ROPs in the BG40H60 flame are quite lower than that in the CH_4 flame due to the coupling effects of H_2 and CO_2. It is thus known that the

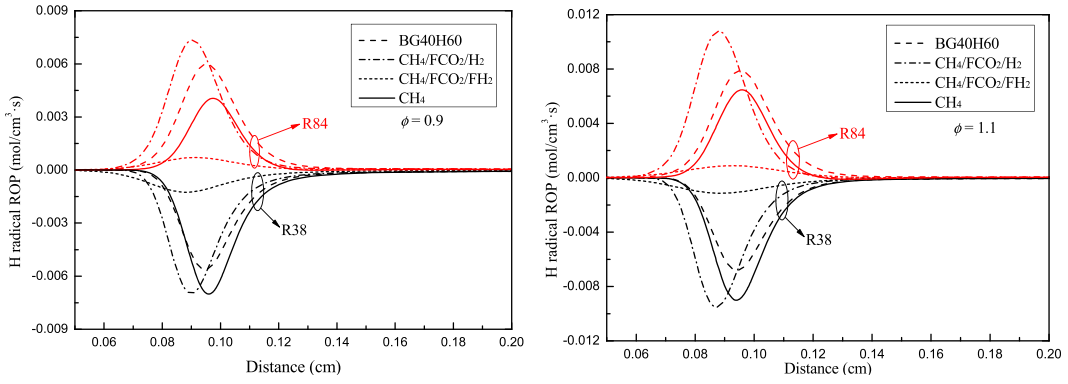

(a) R84 and R38

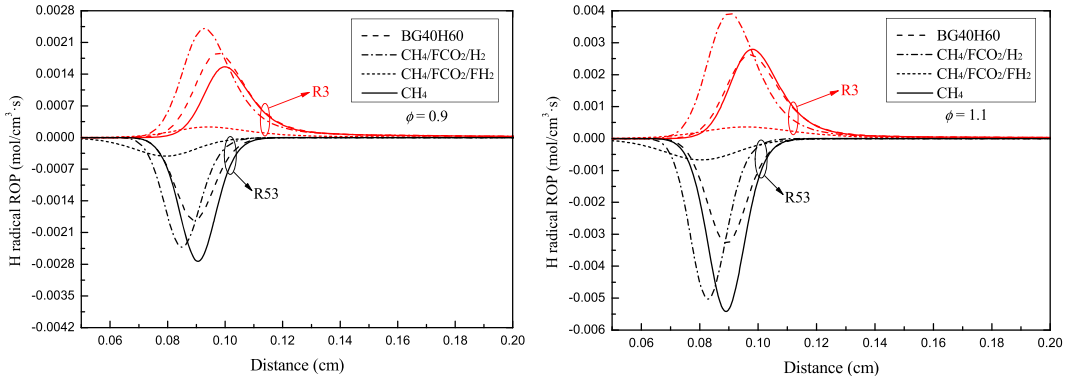

(b) R3 and R53

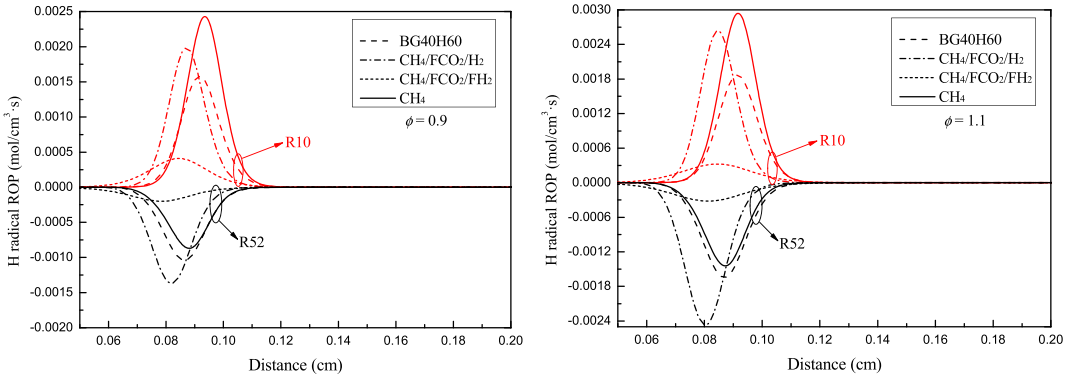

(c) R10 and R52

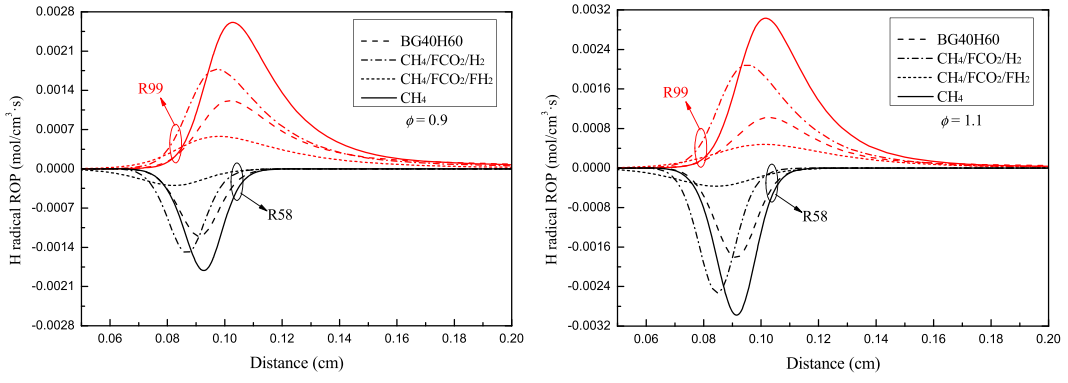

(d) R99 and R58

Fig. 9 – The effects of H_2 and CO_2 on the ROP of H radical in the biogas-hydrogen flames at $\phi = 0.9$ and 1.1.

significances of R84, R3 and R52 on the H radical pool are increased effectively in the biogas-hydrogen flames. R84 and R3 are the H radical production reactions while R52 is the H radical consumption reaction. Considering the ROPs of these reactions, the increased contributions of R84, R3 and R52 means that the positive effects on the H radical pool are improved more effectively than that of negative effects. This consequently contributes to the reduced dropping trend of H radical and laminar flame speed from BG60H40 to BG40H60. Overall, it is known that the H_2 chemical effects dominate the reduced dropping trend of H radical primarily through R84 and R3, which finally leads to the moderate variation of laminar flame speed from BG60H40 to BG40H60 as shown in Fig. 2.

Apart from this, it is noted that CO_2 chemical effects exert more apparent suppressions on the ROPs of these reactions at the fuel-rich condition than that at the fuel-lean condition as shown Fig. 9, which could be attributed to the higher CO_2 concentration at the fuel-rich condition. For example, from $CH_4/FCO_2/H_2$ to BG40H60, the peak ROPs of R84, R3, R38 and R53 are decreased by around 18.6%, 22.8%, 19.5% and 24.4% respectively at the fuel-lean condition due to the CO_2 chemical effects while they are decreased by approximately 27.0%, 33.2%, 28.6% and 35.0% respectively at the fuel-rich condition. For the H radical production, the more evident suppressions of CO_2 chemical effects on the major H radical production reactions (R84, R3, R99 and R10) at the fuel-rich condition can suppress the H radical production more effectively than that at the fuel-lean condition, which can give rise to the decreased concentration of H radical in the flame. In addition, for the H radical consumption reactions, their ROPs are also decreased considerably with the CO_2 chemical effects owing to the direct competition with the large amount of CO_2 in the flame for the H radical. Furthermore, with the stronger CO_2 chemical effects at the fuel-rich condition, the peak ROPs of R53, R52 and R58 are decreased more evidently than that at the fuel-lean condition, which seems to decelerate the consumption of H radical at the fuel-rich condition. Whereas, it is noted that R53, R52 and R58 can play the more significant roles in the H radical consumption at the fuel-rich condition than that at the fuel-lean condition as shown in Fig. 9. Hence, R53, R52 and R58 can still consume the H radical more efficiently at the fuel-rich condition in consideration of their higher contributions on the H radical consumption at fuel-rich condition. This can lead to the more effective consumption of H radical in the BG40H60 flame at the fuel-rich condition than that at the fuel-rich condition. As a result, thanks to the more effective suppressions on the H radical production caused by the more evident CO_2 chemical effects and the more effective H radical consumption due to the increased contributions of the major consumption reactions of H radical, H radical is reduced more evidently at the fuel-rich condition as illustrated in Fig. 6, which then results in the obviously decreased laminar flame speed from CH_4 to BG40H60 at $\phi = 1.1$ as shown in Fig. 2.

Coupling effects on the reaction pathways

In order to further reveal the coupling effects of H_2 and CO_2, main reaction pathways of CH_4 and biogas-hydrogen flames are investigated based on the ROP analysis and results are illustrated in Fig. 10. In the figure, the black arrows denote the primary pathways of CH_4 chemistry while the blue arrows indicate the weakened pathways of CH_4 chemistry in the biogas-hydrogen flame. The major pathways of H_2 chemistry are presented with the red arrows. In addition, CO_2 chemistry is represented by the dash arrow considering that R99 still proceeds in its forward direction in the biogas-hydrogen flame even though the added CO_2 can improve the reverse reaction of R99 considerably. Besides, the pathways whose importance are increased drastically in the biogas-hydrogen flames are highlighted with the red boxes while the pathways with the drastically decreased contributions are highlighted with blue boxes.

In both CH_4 and biogas-hydrogen flames, methane is primarily consumed via the H-abstraction reactions by OH, O and H (R98: $OH + CH_4 = CH_3 + H_2O$, R11: $O + CH_4 = CH_3 + OH$ and R53) to generate the CH_3 radical. In the CH_4 flame, CH_3 radical is mainly consumed via R10, R97: $OH + CH_3 = CH_2(S) + H_2O$, R284: $O + CH_3 = H + H_2 + CO$, R158: $2CH_3(+M) = C_2H_6(+M)$ and R52. Among these reactions, R10, R97 and R284 have the higher contributions on the CH_3 radical consumption at the fuel-lean condition while the significances of R158 and R52 are enhanced at the fuel-rich condition. With the increased amounts of H_2 and CO_2, R10 and R284 still have the stable contributions on the CH_3 consumption in the biogas-hydrogen flames while R97 becomes less important. In addition, the contribution of R52 is enhanced by around 80%, which is resulted from the enhanced collision efficiency by the drastically third-body amount in the flame. As a termination reaction, the increased importance of R52 on the CH_3 radical consumption indicates that the CH_4 consumption is suppressed more effectively with the increased amounts of H_2 and CO_2, which can consequently suppress the flame propagation. The contribution of R158 can reflect the importance of the C_2 pathways in the flame. With the increased H_2 and CO_2 contents, R158 becomes much less important with its contribution dropped by about 40%. This indicates the increasingly important role of the H_2/CO_2-related chemistry in the biogas-hydrogen flame.

Formaldehyde (CH_2O) is primarily produced via R10, which then generate the HCO radical primarily by R101: $OH + CH_2O = HCO + H_2O$ and R58 in both methane and biogas-hydrogen flames. HCO radical can be consumed via various reactions as shown in Fig. 10. In either methane or biogas-hydrogen flame, more than 80% of HCO radical can be consumed via R166: $HCO + H_2O = H + CO + H_2O$, R167: $HCO + M = H + CO + M$ and R168: $HCO + O_2 = CO + HO_2$. R168 plays a more important role at the fuel-lean condition due to the abundant O_2 while the contributions of R167 and R166 are increased at the fuel-rich condition owing to the improved collision efficiency. In addition, with the increased contents of H_2 and CO_2, R168 and R55: $HCO + H = CO + H_2$ have the increased contributions on the HCO radical consumption while the contributions of R166 and R167 are declined steadily. In the biogas-hydrogen flames, CO is still primarily consumed by OH radical via R99. However, the consumption rate of CO is decreased considerably than that in the methane flame owing to the reduced CH_4 and the increased CO_2 in the flame, which can be reflected by the considerably reduced net reaction rate of R99 as shown in Fig. 11.

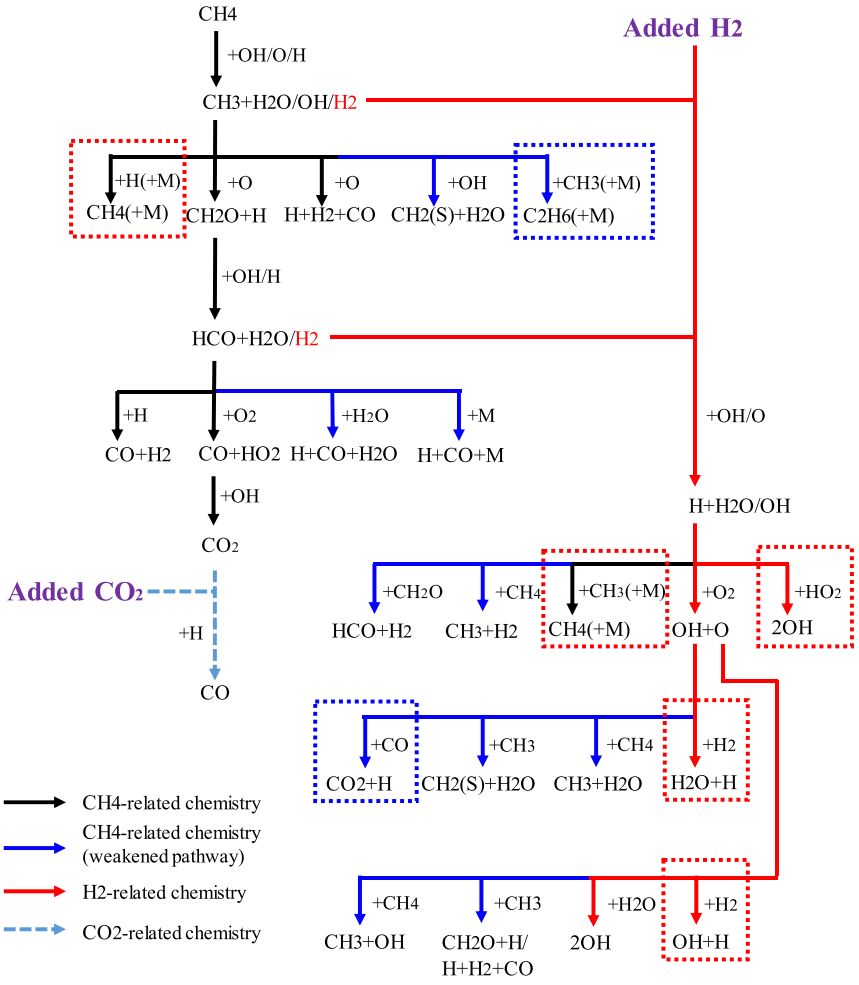

Fig. 10 – Reaction network based on the ROP analysis in the CH_4 and biogas-hydrogen flames.

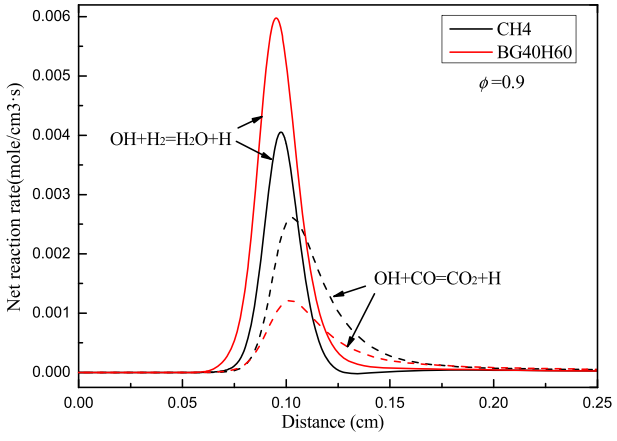

Fig. 11 – Net reaction rates of R84 and R99 in the CH_4 and biogas-hydrogen flames.

H_2 can be produced primarily via R53 and R58 in the methane flame, which is marked with the red font in Fig. 10. Meanwhile, the added H_2 is presented with the purple bold font in Fig. 10. For the H_2, it is primarily consumed by OH and O radicals via R84 and R3 in the methane and biogas-hydrogen flames. R84 is the most important reaction to produce the H radical while R3 is an important chain-branching reaction in the flame. These two reactions can be improved with the increased H_2 and CO_2, which can then make for the flame propagation. H radical can be consumed via various reactions due to its critical role in the flame propagation. In both methane and biogas-hydrogen flame, R38 can account for the largest part of H radical consumption. With the increased contents of H_2 and CO_2, the contributions of R53 and R58 are declined due to reduced CH_4, while the importance of R52 is increased effectively. R53 and R58 are the major reactions to consume H radical in the CH_4 flame, and their declined contributions imply the weakened CH_4-related chemistry. Besides, the increased contribution of R52 further indicates its suppressions on the flame propagation, which confirms its dominated role in the decrease of laminar flame speed of the biogas-hydrogen mixture [33]. By contrast, the contribution of R46: $H + HO_2 = 2OH$ is increased by more than 80% in the biogas-hydrogen flame, which implies the increasingly significant role of H_2-related chemistry.

OH radical is primarily generated via R38 and then reacts with CH_4, CH_3, H_2 and CO primarily to form H_2O and CO_2 in the methane flame. In the biogas-hydrogen flame, the contribution of R84 on the OH radical consumption is enhanced drastically

while that of R97, R98 and R99 are decreased due to the weakened CH_4-related chemistry. For the OH radical consumption, the considerably increased contribution of R84 and drastically decreased contribution of R99 in the biogas-hydrogen flame are highlighted in the red box and blue box respectively as shown in Fig. 10. As the primary oxidization reactions of H_2 and CO, it is general that the net reaction rates of R84 and R99 are enhanced simultaneously with the H_2 addition but decreased simultaneously with the CO_2 addition. Whereas, with the coupling effects of H_2 and CO_2, the net reaction rate of R84 is increased while that of R99 is decreased as shown in Fig. 11. Thanks to the high reactivity and diffusivity of H_2, the increased H_2 concentration leads to the higher flame temperature and the increased amounts of active radicals, which gives rise to the evidently enhanced net reaction rate of R84 and contributes to the improved R99. However, as the same amount of CO_2 is introduced, the reactivity of CO_2 can improve the backward reaction of R99 effectively, which can then overcome the improvements of H_2 and decrease the net reaction rate of R99 finally. In addition, less CO is produced in the biogas-hydrogen flame due to the reduced CH_4 and it needs to compete with H_2 for the OH radical, which can also decelerate the forward reaction of R99 effectively. As a result, the net reaction rate of R99 is decreased considerably with the coupling effects of H_2 and CO_2 as shown in Fig. 11. R84 and R99 can be thus seen as the indicators for the increased importance of H_2/CO_2-related chemistry in the biogas-hydrogen flame.

For the O radical, it is mainly consumed via R3, R10, R11, R86: $O + H_2O = 2OH$ and R284 in the methane and biogas-hydrogen flames. With the increased contents of H_2 and CO_2, the importance of R10, R11 and R284 are decreased owing to the reduced CH_4 concentration while the contribution of R3 is enhanced effectively. This also implies the more important role of H_2-related chemistry in the flame. Overall, it is known that the decreased contributions of R158 and R99 indicate the weakened CH4-related chemistry while R3, R46, R52 and R84 can be seen as the indicator of improved H_2-related chemistry in the biogas-hydrogen flame. Furthermore, coupling effects of H_2 and CO_2 can be monitored directly by the contribution variations of R84 and R99 on the OH radical.

Conclusions

The coupling effects of H_2 and CO_2 on the laminar flame speed and reaction pathways of the biogas-hydrogen mixtures were analyzed using the chemical kinetics simulations. The coupling dilution effects, chemical effects and thermal effects of H_2 and CO_2 were isolated respectively at fuel-lean and fuel-rich conditions in the simulation. The contributions of different effects of H_2 and CO_2 were calculated to identify the dominating factor. The results are summarized as follows:

1. The lower laminar flame speed of biogas-hydrogen mixture is dominated by the coupling dilution effects of H_2 and CO_2, and the more evident dropping trend at the fuel-rich condition is resulted from the more suppressions of CO_2 chemical effects. Furthermore, combined with the stronger suppressions of CO_2 chemical effects at the fuel-rich condition, the more evidently improvements of H_2 chemical effects give rise to the increased and decreased laminar flame speed from BG60H40 to BG40H60 at $\phi = 0.9$ and 1.1, respectively.
2. The variation of laminar flame speed is determined by the variation of H radical in the biogas-hydrogen flame. The coupling dilution effects of H_2 and CO_2 can lead to the considerable decrease in ROP of H radical for all major reactions thanks to the considerably decreased temperature and reduced active radicals. The H_2 chemical effects improve R84 and R3 more effectively, which makes for the more efficient H radical production and increased H radical pool. With the CO_2 chemical effects, the major H radical production reactions of R84, R3, R99 and R10 are suppressed, while R52 plays the more important role in the H radical pool owing to the coupling chemical effects of H_2 and CO_2. This results in the decrease of H radical with the CO_2 chemical effects.
3. Based on the ROP analysis of H radical, it is found that the reduced dropping trends of H radical and laminar flame speed from BG60H40 to BG40H60 are attributed to considerably improved R84 and R3 caused by H2 chemical effects. Besides, with the stronger CO_2 chemical effects at the fuel-rich condition, the more obviously suppressed H radical production reactions and the higher contributions of consumption reactions (R53, R52 and R58) on the H radical pool codetermine the more evident decrease of H radical pool in the biogas-hydrogen flame at the fuel-rich condition than that at the fuel-lean condition.
4. Based on the ROP analysis, R3, R46, R52, R84, R99 and R158 have the primary contributions on the chemistry transition caused by the coupling effects of H_2 and CO_2. The decreased contribution of R158 and R99 indicate the weakened CH_4-related chemistry while the increased contributions of R3, R46, R52 and R84 mean the improved H_2-related chemistry in the biogas-hydrogen flame. Furthermore, the H_2/CO_2–related chemistry can be monitored directly by the contribution variations of R84 and R99 on the OH radical.

Declaration of competing interest

The authors declare that they have no known competing financial interests or personal relationships that could have appeared to influence the work reported in this paper.

Acknowledgement

The Authors thank for the fully financial support from National Natural Science Foundation of China (51766003) and the Scientific research fund of Hai Nan University (KYQD(ZR)1905) to the present project.

REFERENCES

[1] Ju Y, Masuya G, Ronney PD. Effects of radiative emission and absorption on the propagation and extinction of premixed

gas flames. In: Symposium (international) on combustion. Elsevier; 1998. p. 2619–26.
[2] Chao Y-C, Wu C-Y, Lee K-Y, Li Y-H, Chen R-H, Cheng T-S. Effects of dilution on blowout limits of turbulent jet flames. Combust Sci Technol 2004;176:1735–53.
[3] Koroll GW, Kumar RK, Bowles EM. Burning velocities of hydrogen-air mixtures. Combust Flame 1993;94:330–40.
[4] Das LM. Hydrogen-oxygen reaction mechanism and its implication to hydrogen engine combustion. Int J Hydrogen Energy 1996;21:703–15.
[5] Xie Y, Li Q. Effect of the initial pressures on evolution of intrinsically unstable hydrogen/air premixed flame fronts. Int J Hydrogen Energy 2019;44:17030–40.
[6] Wang J, Li Y, Xia H, Ju R, Zhang M, Mu H, et al. Effect of hydrogen enrichment and electric field on lean CH4/air flame propagation at elevated pressure. Int J Hydrogen Energy 2019;44:15962–72.
[7] Briones AM, Aggarwal SK, Katta VR. Effects of H2 enrichment on the propagation characteristics of CH4–air triple flames. Combust Flame 2008;153:367–83.
[8] Miao J, Leung CW, Cheung CS. Effect of hydrogen percentage and air jet Reynolds number on fuel lean flame stability of LPG-fired inverse diffusion flame with hydrogen enrichment. Int J Hydrogen Energy 2014;39:602–9.
[9] Huzayyin AS, Moneib HA, Shehatta MS, Attia AMA. Laminar burning velocity and explosion index of LPG–air and propane–air mixtures. Fuel 2008;87:39–57.
[10] Xie Y, Sun ZY. Effects of the external turbulence on centrally-ignited spherical unstable Ch4/H2/air flames in the constant-volume combustion bomb. Int J Hydrogen Energy 2019;44:20452–61.
[11] Zhang W, Wang J, Lin W, Mao R, Xia H, Zhang M, et al. Effect of differential diffusion on turbulent lean premixed hydrogen enriched flames through structure analysis. Int J Hydrogen Energy 2020;45(18):10920–31.
[12] Guo S, Wang J, Zhang W, Zhang M, Huang Z. Effect of hydrogen enrichment on swirl/bluff-body lean premixed flame stabilization. Int J Hydrogen Energy 2020.
[13] Leung T, Wierzba I. The effect of hydrogen addition on biogas non-premixed jet flame stability in a co-flowing air stream. Int J Hydrogen Energy 2008;33:3856–62.
[14] Chen S, Zheng C. Counterflow diffusion flame of hydrogen-enriched biogas under MILD oxy-fuel condition. Int J Hydrogen Energy 2011;36:15403–13.
[15] Xin Z, Jian X, Shizhuo Z, Xiaosen H, Jianhua L. The experimental study on cyclic variation in a spark ignited engine fueled with biogas and hydrogen blends. Int J Hydrogen Energy 2013;38:11164–8.
[16] Hu Z, Zhang X. Experimental study on flame stability of biogas/hydrogen combustion. Int J Hydrogen Energy 2019;44:5607–14.
[17] Wei ZL, Leung CW, Cheung CS, Huang ZH. Effects of H2 and CO2 addition on the heat transfer characteristics of laminar premixed biogas–hydrogen Bunsen flame. Int J Heat Mass Tran 2016;98:359–66.
[18] Zhen HS, Leung CW, Cheung CS, Huang ZH. Characterization of biogas-hydrogen premixed flames using Bunsen burner. Int J Hydrogen Energy 2014;39:13292–9.
[19] Zhen HS, Wei ZL, Chen ZB, Xiao MW, Fu LR, Huang ZH. An experimental comparative study of the stabilization mechanism of biogas-hydrogen diffusion flame. Int J Hydrogen Energy 2019;44:1988–97.
[20] Wei ZL, Leung CW, Cheung CS, Huang ZH. Effects of equivalence ratio, H2 and CO2 addition on the heat release characteristics of premixed laminar biogas-hydrogen flame. Int J Hydrogen Energy 2016;41:6567–80.
[21] Wei ZL, Zhen HS, Leung CW, Cheung CS, Huang ZH. Experimental and numerical study on the emission characteristics of laminar premixed biogas-hydrogen impinging flame. Fuel 2017;195:1–11.
[22] Wei Z, Zhen H, Leung C, Cheung C, Huang Z. Effects of H2 addition on the formation and emissions of CO/NO2/NOx in the laminar premixed biogas-hydrogen flame undergoing the flame-wall interaction. Fuel 2020;259:116257.
[23] Wei Z, Zhen H, Leung C, Cheung C, Huang Z. Effects of unburned gases velocity on the CO/NO2/NOx formations and overall emissions of laminar premixed biogas-hydrogen impinging flame. Energy 2020;196:117146.
[24] Zheng L, Dou Z, Du D, Wang X, Jin H, Yu M, et al. Study on explosion characteristics of premixed hydrogen/biogas/air mixture in a duct. Int J Hydrogen Energy 2019;44:27159–73.
[25] Hu Z, Wang Y, Zhang J, Hou X. Experimental study on self-acceleration characteristics of unstable flame of low calorific value gas blended with hydrogen. Int J Hydrogen Energy 2019;44:25248–56.
[26] Bouguessa R, Tarabet L, Loubar K, Belmrabet T, Tazerout M. Experimental investigation on biogas enrichment with hydrogen for improving the combustion in diesel engine operating under dual fuel mode. Int J Hydrogen Energy 2020;45:9052–63.
[27] Hou XS, Zhang X, Hu ZQ. Experimental and numerical study on engine fueled with different fractions of natural gas–carbon dioxide-hydrogen blends. Int J Hydrogen Energy 2019;44:5599–606.
[28] Park C, Park S, Kim C, Lee S. Effects of EGR on performance of engines with spark gap projection and fueled by biogas–hydrogen blends. Int J Hydrogen Energy 2012;37:14640–8.
[29] Khatri N, Khatri KK. Hydrogen enrichment on diesel engine with biogas in dual fuel mode. Int J Hydrogen Energy 2020;45:7128–40.
[30] Hu Z, Zhang X. Study on laminar combustion characteristic of low calorific value gas blended with hydrogen in a constant volume combustion bomb. Int J Hydrogen Energy 2019;44:487–93.
[31] Kumar Yadav V, Ray A, Ravi MR. Experimental and computational investigation of the laminar burning velocity of hydrogen-enriched biogas. Fuel 2019;235:810–21.
[32] Pizzuti L, Martins CA, Lacava PT. Laminar burning velocity and flammability limits in biogas: a literature review. Renew Sustain Energy Rev 2016;62:856–65.
[33] Wei Z, Zhen H, Fu J, Leung C, Cheung C, Huang Z. Experimental and numerical study on the laminar burning velocity of hydrogen enriched biogas mixture. Int J Hydrogen Energy 2019;44:22240–9.
[34] Zhang K, Jiang X. An assessment of fuel variability effect on biogas-hydrogen combustion using uncertainty quantification. Int J Hydrogen Energy 2018;43:12499–515.
[35] Kee Jfg RJ, Smooke MD, Miller JA. A FORTRAN program for modeling steady, laminar, one-dimensional premixed flames. Sandia National Laboratories; 1993. SNAD85–8240.
[36] Gregory P. Smith DMG, Michael Frenklach, Nigel W. Moriarty, Boris Eiteneer, Mikhail Goldenberg. GRI 3.0. http://wwwmeberkeleyedu/gri_mech.
[37] Zhang X, Mei B, Ma S, Pan H, Wang H, Li Y. Experimental and kinetic modeling investigation on laminar flame propagation of CH4/CO mixtures at various pressures: insight into the transition from CH4-related chemistry to CO-related chemistry. Combust Flame 2019;209:481–92.
[38] Liu F, Guo H, Smallwood GJ. The chemical effect of CO2 replacement of N2 in air on the burning velocity of CH4 and H2 premixed flames. Combust Flame 2003;133:495–7.

[39] Xie M, Fu J, Zhang Y, Shu J, Ma Y, Liu J, et al. Numerical analysis on the effects of CO2 dilution on the laminar burning velocity of premixed methane/air flame with elevated initial temperature and pressure. Fuel 2020;264:116858.

[40] Nonaka HOB, Pereira FM. Experimental and numerical study of CO2 content effects on the laminar burning velocity of biogas. Fuel 2016;182:382–90.